PLOS ONE

RESEARCH ARTICLE

# Identification of candidate genes for developmental colour agnosia in a single unique family

**Tanja C. W. Nijboer[1,2☯], Ellen V. S. Hessel[1,3☯], Gijs W. van Haaften[3☯], Martine J. van Zandvoort[2], Peter J. van der Spek[4], Christine Troelstra[4], Carolien G. F. de Kovel[3], Bobby P. C. Koeleman[3], Bert van der Zwaag[3], Eva H. Brilstra[3], J. Peter H. Burbach[5]***

**1** UMCU Brain Center and Center of Excellence for Rehabilitation Medicine, University Medical Center Utrecht and De Hoogstraat Rehabilitation, Utrecht, The Netherlands, **2** Department of Experimental Psychology and Helmholtz Institute, Utrecht University, Utrecht, The Netherlands, **3** Department of Biomedical Genetics, University Medical Center Utrecht, Utrecht, The Netherlands, **4** Department of Pathology, Erasmus Medical Center Rotterdam, Rotterdam, the Netherlands, **5** UMCU Brain Center, Department of Translational Neuroscience, University Medical Center Utrecht, Utrecht, the Netherlands

☯ These authors contributed equally to this work.
* j.p.h.burbach@umcutrecht.nl





**Citation:** Nijboer TCW, Hessel EVS, van Haaften GW, van Zandvoort MJ, van der Spek PJ, Troelstra C, et al. (2023) Identification of candidate genes for developmental colour agnosia in a single unique family. PLoS ONE 18(9): e0290013. https://doi.org/10.1371/journal.pone.0290013

**Editor:** Nejat Mahdieh, Shaheed Rajaei Hospital: Rajaie Cardiovascular Medical and Research Center, ISLAMIC REPUBLIC OF IRAN

**Received:** June 30, 2023

**Accepted:** July 31, 2023

**Published:** September 6, 2023



**Data Availability Statement:** All meta data of this study are being presented in this manuscript. Providing data on individuals in this study are restricted due to legal and ethical rules. We have provided contacts for data inquiries in the form of one of the investigators (G.vanhaaften@umcutrecht.nl) as well as the data management team of our institution (onderzoekdivisiehersenen@umcutrecht.nl).

## Abstract

Colour agnosia is a disorder that impairs colour knowledge (naming, recognition) despite intact colour perception. Previously, we have identified the first and only-known family with hereditary developmental colour agnosia. The aim of the current study was to explore genomic regions and candidate genes that potentially cause this trait in this family. For three family members with developmental colour agnosia and three unaffected family members CGH-array analysis and exome sequencing was performed, and linkage analysis was carried out using DominantMapper, resulting in the identification of 19 cosegregating chromosomal regions. Whole exome sequencing resulted in 11 rare coding variants present in all affected family members with developmental colour agnosia and absent in unaffected members. These variants affected genes that have been implicated in neural processes and functions (*CACNA2D4*, *DDX25*, *GRINA*, *MYO15A*) or that have an indirect link to brain function, development or disease (*MAML2*, *STAU1*, *TMED3*, *RABEPK*), and a remaining group lacking brain expression or involved in non-neural traits (*DEPDC7*, *OR1J1*, *OR8D4*). Although this is an explorative study, the small set of candidate genes that could serve as a starting point for unravelling mechanisms of higher level cognitive functions and cortical specialization, and disorders therein such as developmental colour agnosia.

## Introduction

Genetics of developmental disorders of the human brain has been a main strategy to uncover biological mechanisms of brain development and functioning. In particular, understanding of the development of the cerebral cortex has benefited from the recognition of specific cortical abnormalities and the elucidation of causative gene defects [1–3]. Genetic aberrations in

**Funding:** This project was supported financially by the Neuroscience Center Utrecht as part of the intramural Focus & Massa programme grant of the Utrecht University to JPHB. The funder had no role in study design, data collection and analysis, decision to publish, or preparation of the manuscript.

**Competing interests:** The authors have declared that no competing interests exist.

cortical specializations may be a treasure trove to find genetic dominators and mechanisms of cognitive functions [4, 5].

Different disorders of cortical specialization have been described (reviewed by [4]: prosopagnosia (i.e. inability to recognise faces/people despite normal intelligence), synesthesia (i.e. stimulation of one sensory or cognitive pathway leads to automatic, involuntary experiences in a second sensory or cognitive pathway, for example, letters or numbers are perceived as inherently coloured), dyslexia (i.e. disability in reading despite normal intelligence), and congenital amusia (i.e. defect in processing pitch, but may also include musical memory and recognition).

In this study we focussed on a very rare disorder of cortical specialization, namely developmental colour agnosia. Disorders of colour processing have been reported at different levels, ranging from wavelength processing deficits up to very specific impairments in object-colour associations [6]. One of the most intriguing disorders may be colour agnosia. In colour agnosia, people have intact colour perception, yet have severe difficulties in naming, categorising, and recognising colours and form adequate object-colour associations [7–9]. In most cases, colour agnosia is acquired after brain damage, either bilateral or left hemisphere lesions [10], mostly in the occipitotemporal lobe [6].

Over a decade ago we reported the first and only case of developmental colour agnosia [9]. Additionally, a familial factor in developmental colour agnosia was described when family members in three generations also showed difficulties in colour naming and recognition [7], indicating a genetic origin of the trait. The affected individuals of this family all display normal cognition and intact colour perception at a visuosensory level, e.g. matching of equiluminant colours. However, they could not name colours, match colour names to colours, categorise hues into general clusters of colour or point a colour that is mentioned by the examiner [11]. This trait likely is a disorder in cortical specialization [4]. Such disorders may have a genetic origin resulting in abnormal cortical development.

In order to identify genetic origins and to gain more insight into the developmental mechanisms related to these disorders, we analyzed all participating members of this family by CGH-arrays and whole-exome sequencing. The results reveal a small set of extremely rare variants that are candidate to cause developmental colour agnosia within the limits of this study.

## Subjects and methods

### Subjects and DNA isolation

Informed and written consent were obtained from the family members to perform DNA analysis and sequencing, and to publish results in a scientific paper as approved by the Medical Ethical Committee of the University Medical Center Utrecht by METC protocol number 12–222. Four members were phenotyped earlier [7]. For this study, two additional family members were tested and diagnosed with or without developmental colour agnosia. Phenotyping has been described by [7, 11]. In total three affected (age 78, 51 and 13) and three unaffected family members (46, 12 and unknown adult) were available for this study (Fig 1). The individuals were recruited in this study in 2010 and 2011. Genomic DNA of the six family members was isolated from saliva using the QIAamp® DNA Blood Mini Kit (Qiagen) with the supplementary protocol for isolation of genomic DNA from saliva and mouthwash as provided by the company. The DNA concentration was determined by using Qubit Quant-IT (Invitrogen). The authors TCWN, EVSH, GWvH, MJvZ, EHB and JPHB had access to information that could identify individual participants during or after data collection. Data contacts are g.van-haaften@umcutrecht.nl and onderzoekdivisiehersenen@umcutrecht.nl.

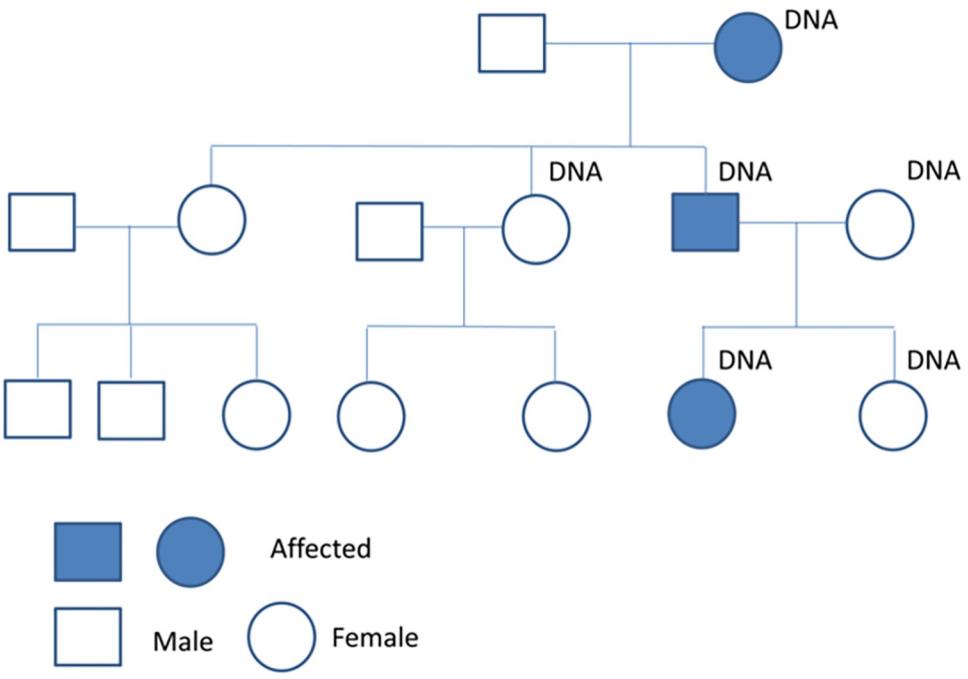


**Fig 1. Family with developmental colour agnosia.** DNA means that these family members underwent genetic analysis. Three affected persons are indicated (filled dark blue).

https://doi.org/10.1371/journal.pone.0290013.g001

## Array-based comparative genomic hybridization and linkage analysis

Array-CGH microarray analysis was performed using 105K (Agilent amadid 019015, hg18) microarray slides from Agilent Technologies (Santa Clara, CA) following manufacturer's protocols and a mixed pool of either 50 healthy males or females was used as a reference. Scanned images were analyzed by Feature Extraction software (Agilent Technologies). Data analysis was performed using DNA analytics 4.76 Software from Agilent Technologies using the ADM-2 algorithm. Interpretation of CNV-data was performed as described in the guidelines of [12]. Copynumber variations and sequence homologies flanking the breakpoints were confirmed using the Database of Genomic Variation (http://www.projects.tcag.ca/variation/) and the UCSC Genome Browser (http://www.genome.ucsc.edu/index) [13].

Linkage analysis was performed by using the array CGH chromosome profiles and mapping of the disease loci was calculated with DominantMapper [14]. This program calculated which chromosomal regions are present in all affected family members and not present in all non-affected family members based on SNP genotyping data.

## Library preparation and whole exome sequencing

DNA (2ug) was used for the preparation of a barcoded fragment library [15]. This was followed by multiplexed enrichment and sequencing on the SOliD Next-generation sequencing platform containing the exonic sequences of ~18.000 genes and covering a total of ~37Mb of genomic sequence [15, 16]. In brief, genomic DNA was fragmented using the Covaris S2 System (Applied Biosystems) to 100–150-bp fragments with a mean size of 125 bp using the following settings: number of cycles, 3; bath temperature, 4˚C; bath temperature limit, 8˚C; mode, frequency sweeping; duty cycle, 20%; intensity, 5; cycles/burst, 200; and time per cycle, 1 min 45 seconds. After fragmentation, the DNA was end repaired and phosphorylated at the

5′ end using the End-It DNA End-Repair Kit (EpiCenter) and purified with the Agencourt AMPure XP system (Beckman Coulter Genomics). DNA was then ligated to double-stranded truncated adaptors compatible with the SOLiD next-generation sequencing platform using the Quick Ligation Kit (NEB). After purification, each sequencing library was nick translated, barcoded and amplified in a single PCR assay. The intensity of library bands was examined on a 2% agarose gel (Lonza FlashGel System). Amplified library fragments in the range of 175–225 bp in size were selected on a 4% agarose gel and purified using a QIAquick Gel Extraction Kit (Qiagen). Libraries from the family members were pooled in equimolar concentrations and were enriched using the Agilent SureSelect Human All Exon 50Mb Kit (Agilent Technologies). Enriched library pool fragments were amplified using 12 PCR cycles and elongated to a full-length adaptor sequence required for SOLiD sequencing. SOLiD sequencing was performed according to the instructions in the SOLiD 4 manual to produce enough 50-bp reads to obtain sufficient coverage for a single allele in each library.

## Variant detection and exome sequencing analysis

Raw sequencing reads were mapped against the human reference genome GRCh37/hg19 using our custom pipeline based on the Burrows-Wheeler Alignment (BWA) algorithm26. Sequence data were submitted to the EMBL-EBI Sequence Read Archive (see URLs). Single-nucleotide variants (SNVs) and small indels ($\leq$7 nt) were called by our custom analysis pipeline as described [17]. All scripts are available upon request. The criteria for variant detection were set to enable discovery of heterozygous variants, since we assume dominant inheritance. We required that variants should minimally be supported by two read seeds (first 25 bp, the higher quality portion of a read), and we set the cut-off for coverage to a minimum of ten reads and the cutoff for non-reference allele percentage to 15%. Since it is probably a dominant inherited phenotype, we set the cut-off for non-reference allele percentage to a maximum of 80%. A maximum of five clonal reads (defined as reads with an identical start site) were included in the analysis. Only truncating variants including nonsense frameshifting insertions or deletions, or missense and splice site alterations were selected. All polymorphisms with an allele frequency $< 0.002$ in the different databases in EVS database (http://evs.gs.washington.edu/EVS/)), Exac (http://exac.broadinstitute.org/) or GoNL (http://www.nlgenome.nl/) were excluded, and variants present in our in-house database $>$ 0,1,2 x present were excluded from analysis; For each variant, the genomic location, amino-acid change, effect on protein function, conservation score and output from prediction programs (Polyphen, Polyphen-2, SIFT and Condel) were compiled [15]. Alamut was used to study the variants in more detail. Prioritization and variant selection is described in Fig 2. Identified variants were confirmed with Sanger sequencing.

## Gene expression analyses

Comprehensive human brain transcriptome data sets were used to determine the developmental expression profiles of all candidate genes [18]. The set contains the age-related expression in 39 samples of the dorsolateral prefrontal cortex from individuals ranging from 0.1 to 83 years of age (Gene Logic Inc, Gaithersburg, MD, USA, [18, 19]). Raw data of these studies were available online as GEO entry (GSE11882, Fig 3).

For analysis of gene expression single-cell RNAseq datasets provided by the Allen Brain Institute were used in the Allen Brain Map Transcriptomics Explorer (https://portal.brain-map.org). For the human brain on datasets Human-M1-10X and Human-Multiple cortical areas-SMART-seq were used [20]. For the mouse brain the data set Mouse-Whole mouse brain & hippocampus-10X was used. In addition, data of the mouse cortex [21, 22] were mined through the Single Cell Portal (https://singlecell.broadinstitute.org/single_cell) and the

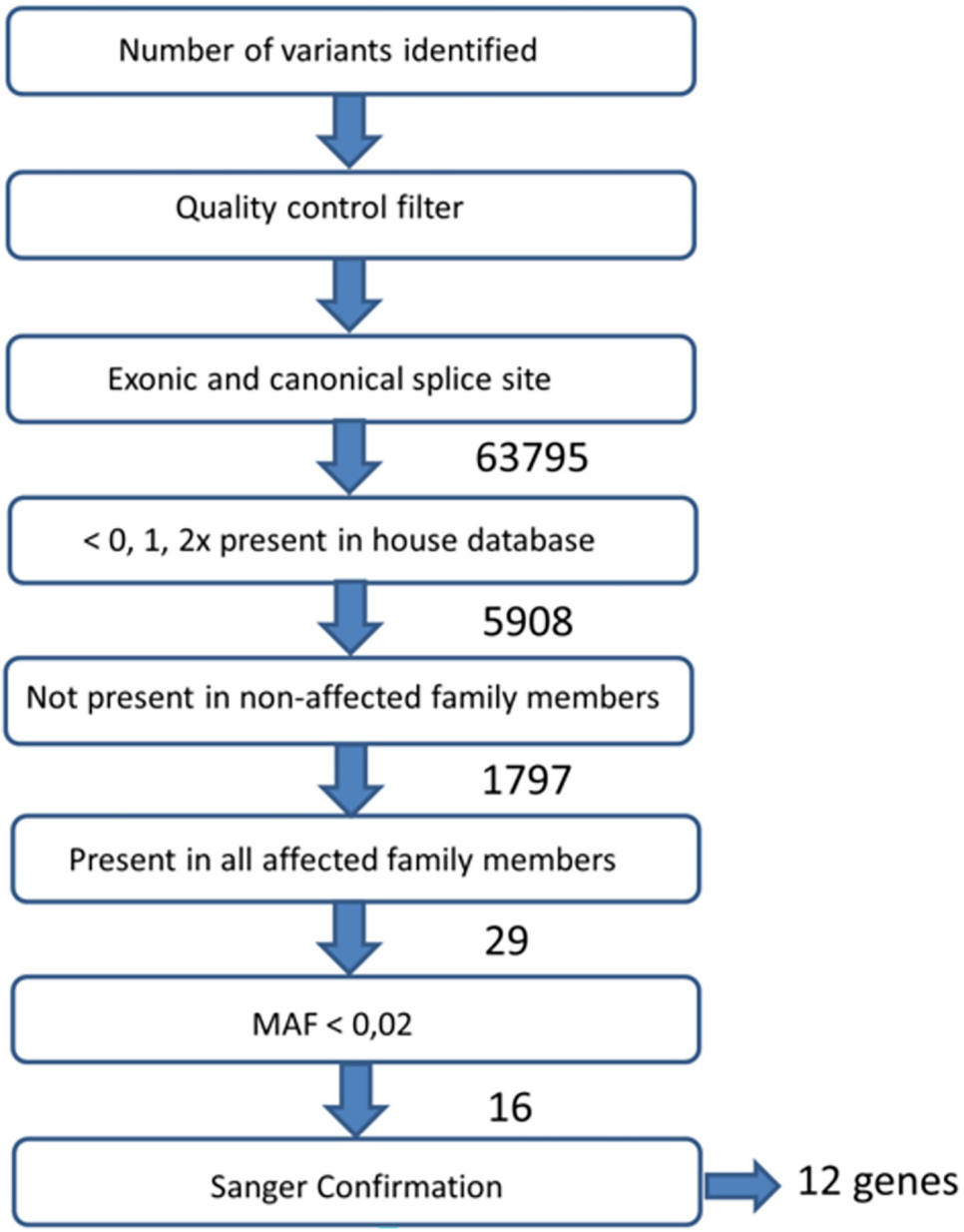


**Fig 2. Selection of variants cosegregating with developmental colour agnosia based on whole exome sequencing.** Selection is based on the presence of the mutation in the affected family members and the absence in the unaffected family members.

https://doi.org/10.1371/journal.pone.0290013.g002

Allen Brain Atlas data portal (http://casestudies.brain-map.org/celltax#section_explorea). The Mouse Brain Atlas and Developing Mouse Brain Atlas were used for anatomical analysis of gene expression (https://portal.brain-map.org).

## Results

### CGH-array and linkage analysis

Segregration patterns of developmental colour agnosia in the family are most consistent with Mendelian dominant inheritance (Fig 1). Array CGH performed on the six family members

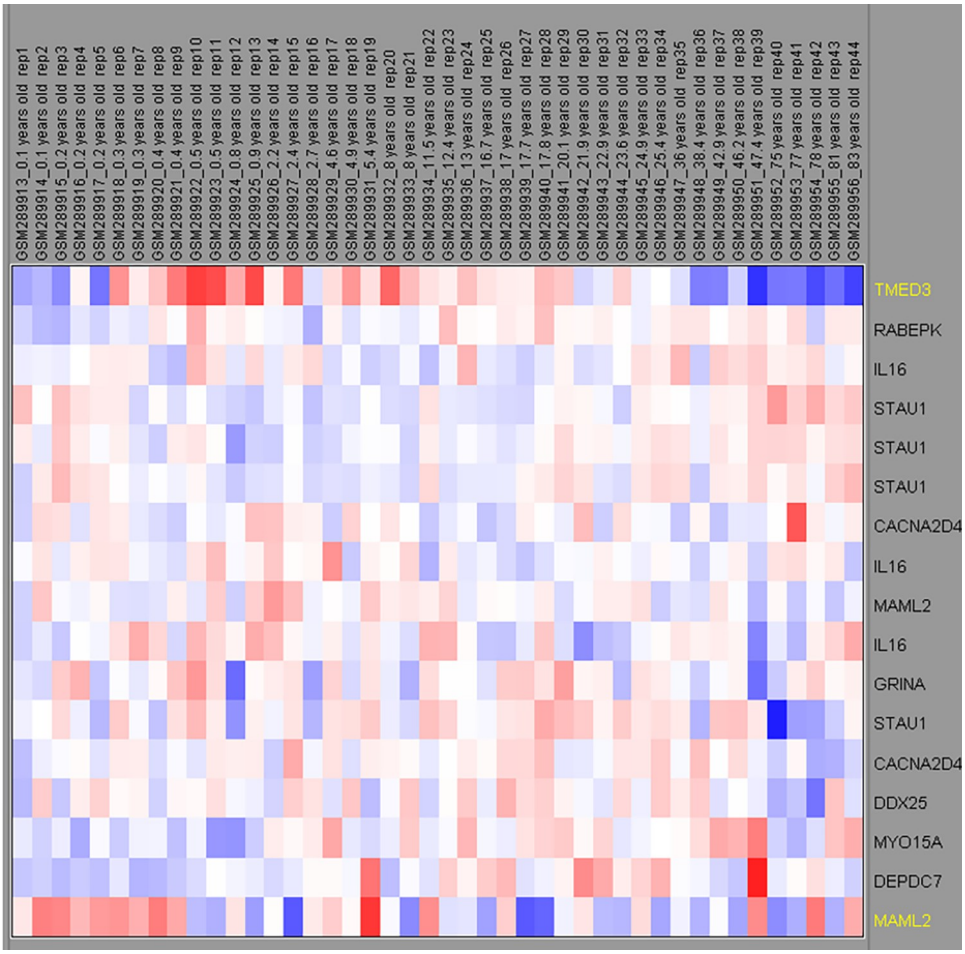


**Fig 3. Relative expression of the candidate genes in the human brain (prefrontal cortex) during development.** The upper lane describes the age of the brain samples and sample ID. The gene names are mentioned at the right. The colour scheme of the boxes relate to the relative expression level of gene transcripts using a log2 normalized expression map where the colour scale ranges from dark blue (low expression) to dark red (high expression).

https://doi.org/10.1371/journal.pone.0290013.g003

showed that there are no large chromosomal rearrangements co-segregating with the phenotype of developmental colour agnosia. Next, we performed linkage analysis on SNP data to identify loci cosegregating with developmental colour agnosia. All family members were included in the linkage analysis assuming an autosomal dominant model of inheritance. The genome wide linkage resulted in the identification of multiple linked chromosomal regions (Table 1). These linked regions were used for the identification of the candidate genes assuming that the causal gene will be present in a linked region.

## Exome sequencing and candidate gene selection

We hypothesized that developmental colour agnosia is caused by a single heterozygous rare non-synonymous variant present in all affected family members and absent in unaffected family members. Candidate gene selection was performed by filtering as described in Fig 2. Exome sequencing followed by quality control identified in total in all family members 63795 variants present in exons and canonical splice sites. Of these, 5908 variants were protein truncating with putative loss of function alteration, including nonsense frameshift (indels) or splice site variants, and were *de novo* or rare in the population (0, 1, 2 times present in the in-house

**Table 1. Linked chromosomal regions to colour agnosia.**

| Chr. | Locus | Start | End | Length |
|---|---|---|---|---|
| 2 | 2q22.3–35 | 146360626 | 221800201 | 75439575 |
| 3 | 3p11.2-q11.2 | 87373894 | 94512868 | 7138974 |
| 3 | 3q13.3-q25.31 | 119442572 | 159239866 | 39797294 |
| 4 | 4q13.1-4q22.3 | 60013919 | 96704454 | 36690535 |
| 5 | 5p15.33-5p15.2 | 2346621 | 10752315 | 8405694 |
| 6 | 6q26-27 | 162736476 | 168554222 | 5817746 |
| 8 | 8q24.23–24.3 | 138970102 | 143270729 | 4300627 |
| 8 | 8p22-q13.1 | 14253354 | 68723609 | 54470255 |
| 9 | 9q21.32-q34.11 | 83858558 | 138149166 | 54290608 |
| 10 | 10p15.3-p14 | 135708 | 8638235 | 8502527 |
| 11 | 11p14.3-q24 | 21234023 | 128206410 | 106972387 |
| 12 | 12p13-q23.3 | 661031 | 67262352 | 66601321 |
| 14 | 14q12-q31.2 | 22645683 | 88752821 | 66107138 |
| 15 | 15q15.1-q26.1 | 40509600 | 94077313 | 53567713 |
| 17 | 17p12-q25.3 | 9078327 | 77698582 | 68620255 |
| 19 | 19p12-q21 | 23446279 | 28836326 | 5390047 |
| 20 | 20q13.13-q13.33 | 47050483 | 60111743 | 13061260 |
| 21 | 21q11.2-q22.12 | 14687571 | 38082812 | 23395241 |
| 22 | 22q11.2-q13.2 | 16079545 | 44595591 | 28516046 |

Chromosomal regions linked to developmental colour agnosia (hg19). These haplotypes of these regions are present in all affected individuals and absent in the non-affected individuals.

https://doi.org/10.1371/journal.pone.0290013.t001

database). Of these 5908 variants, 1797 were not present in non-affected family members and 29 were present in all three affected family members. Of these 29 variants we further studied the frequency of these variants, to assume that the variants are rare or *de novo* in a broader population. Based on frequency of presence in the Exome Variant Server (EVS) database (frequency 0:13000–25:13000 (frequency $< 0.002$)) (n = 17) and Variance GoNL database (24) (n = 16), and confirmation of the variant in the linked region by Sanger sequencing (n = 11), 11 candidate variants in 11 genes remained (Table 2). These were: *GRINA* (glutamate receptor, ionotropic, N-methyl D-aspartate-associated protein 1), *OR1J1* (olfactory receptor, family 1, subfamily J, member 1), *RABEPK* (Rab9 effector protein with Kelch motifs), *DEPDC7* (DEP domain containing 7), *MAML2* (mastermind-like 2 (Drosophila)), *OR8D4* (olfactory receptor, family 8, subfamily D, member 4), *DDX25* (DEAD (Asp-Glu-Ala-Asp) box polypeptide 25), *CACNA2D4* (calcium channel, voltage-dependent, alpha 2/delta subunit 4), *TMED3* (trans-membrane emp24 protein transport domain containing 3), *IL16* (interleukin 16), *MYO15A* (myosin XVA), *STAU1* (staufen double-stranded RNA binding protein 1). Additional information including allele frequency in the 1000 Genome Project [23] (The 1000 Genomes Project Consortium), Variance GoNL [24, 25] and Wellderly cohort [26] is presented in Table 3.

## Effect of the mutation

Prediction about the effect of the mutations were made by three software packages: Polyphen, Polyphen-2, SIFT and Condel (Table 3). Two variants (*GRINA* and *RABEPK*) were predicted to be probably damaging (Polyphen) and deletious (SIFT). Six variants (*OR1J1*, *DEPDC7*, *MAML2*, *DDX25*, *TMED3*, *STAU1*) were predicted as tolerated by SIFT; some of these were benign or possibly damaging by Polyphen (*OR1J1*, *DDX25*, *DEPDC7*, *TMED3*, *STAU1*).

**Table 2. Properties of selected candidate genes.**

| Genome position (hg19) | Nucleotide change | Gene symbol | Ensemble transcript | Consequence | Amino acid change | SNP id | Allele Frequency (GnomAD v2.1.1) | Protein function |
|---|---|---|---|---|---|---|---|---|
| 8_145066215 | G/A | *GRINA* | ENST00000313269 | NS | R221Q | novel | 2/282710 | Glutamate Receptor |
| 9_125239752 | C/T | *OR1J1* | ENST00000259357 | NS | A152T | rs143862742 | 4/281994 | Olfactory receptor |
| 9_127990266 | G/A | *RABEPK* | ENST00000373538 | NS | G202R | rs142347258 | 80/278552 | RAB9 effector protein |
| 11_33052944 | C/T | *DEPDC7* | ENST00000241051 | NS | A268V | novel | 0/249446 | G-protein signalling DEP domain |
| 11_95712527 | T/C | *MAML2* | ENST00000524717 | NS | Q1019R | rs201299551 | 95/279812 | Transcriptional Coactivator Notch |
| 11_123777296 | G/A | *OR8D4* | ENST00000321355 | NS | R53H | rs201007236 | 224/282640 | Olfactory receptor |
| 11_125786960 | C/G | *DDX25* | ENST00000263576 | NS | D284E | rs370049057 | 3/241854 | DEAD box RNA helicase |
| 12_1949897 | G/A | *CACNA2D4* | ENST00000382722 | SS | NA | rs376597005 | 9/280408 | Calcium Channel |
| 15_79614380 | C/T | *TMED3* | ENST00000299705 | NS | H160Y | novel | 3/282836 | Transmembrane protein |
| 17_18043906 | C/T | *MYO15A* | ENST00000205890 | NS | R1763W | rs200146361 | 513/280690 | Actin based motor molecule |
| 20_47740944 | T/C | *STAU1* | ENST00000371856 | NS | R264G | rs201180807 | 32/282876 | RNA binding protein |

All variants segregate in the heterozygous state in all affected color agnosia individuals and absent in family members without color agnosia. NS: non-synonymous mutation. SS: mutation changing a splice site.

https://doi.org/10.1371/journal.pone.0290013.t002

*MAML2* was predicted as probably damaging by Polyphen. *OR8D4* was deleterious on SIFT and benign on Polyphen. MYO15A was probably damaging by Polyphen and undefined by SIFT. The effects of two variants (*IL16* and *CACNA2D4)* could not be predicted, since these are splice site mutations (Table 2).

## Gene expression during human brain development

We have attempted to prioritize the 11 candidate genes for a possible role in developmental colour agnosia. For all these genes, we have analyzed (developmental) brain expression (Fig 3). We hypothesised cortical expression during development for a gene linked to developmental colour agnosia and possible increased expression during postnatal brain maturation. For that reason we first studied expression of the 11 candidate genes in the human brain of subjects free of neurological disorders, in the age range of 0.1 to 83 years, represented by the Ingenuity data set. All genes seem to be expressed in the brain, while two genes, *TMED3* and *MAML2*, displayed an increased expression during development (*TMED3*, 0.4–2.4 years old and *MAML2*, 0.1–2.4; Fig 3). The other nine genes do not show a clear expression profile during a specific developmental age window.

Mining of single-cell transcriptomic data of the adult human cortex and mouse brain showed that MAML2 was the only gene that maintained expression at high levels, albeit restricted to only a limited number of cell types (Fig 4). The other genes displayed a low to very low level of expression (*GRINA*, *RABEPK*, *DDX25*, *CACNA2D4*, *STAU*1) or no expression. In the human M1 motor cortex *MAML2* was expressed by three types of inhibitory interneurons, one type of excitatory neuron, and by no-neuronal cells: astrocytes, an olfactory progenitor neuron and microglia (Fig 4). In this respect it was de only gene that was expressed by non-neuronal cells. In the mouse cortex and hippocampus *Mam*l2 was also expressed in a very restricted set of neurons (dentate gyrus and CA3) and in non-neuronal cells. *Grina* and *Stau1* displayed wide, but low expression in inhibitory and excitatory neurons (Fig 4).

**Table 3. Variant frequencies and mutation prediction.**

| Gene_name | Frequencies | | | Effect of mutation | | | | | Conservation (Condel) | |
|---|---|---|---|---|---|---|---|---|---|---|
| | EVS | GoNL | Exac | Effect | Polyphen_s | Polyphen_p | SIFT_s | SIFT_p | Conserved Nucl | Conserved AA |
| *GRINA* | 1/13005 | 0 | 0/121000 | NS | 1 | probably damaging | 0 | deleterious | highly | highly |
| *OR1J1* | 0 | 0 | 1/120930 | NS | 0.001 | benign | 0.56 | tolerated | weakly | highly |
| *RABEPK* | 11/12995 | 2/996 | 36/120704 | NS | 1 | probably damaging | 0 | deleterious | highly | highly |
| *DEPDC7* | 0 | 0 | 0/120000 | NS | 0.896 | possibly damaging | 0.07 | tolerated | moderately | moderately |
| *MAML2* | 1/12217 | 0 | 50/119130 | NS | 0.998 | probably damaging | 0.06 | tolerated | moderately | highly |
| *OR8D4* | 6/12996 | 1/996 | 102/121352 | NS | 0 | benign | 0 | deleterious | weakly | weakly |
| *DDX25* | 1/12537 | 1/996 | 3/76840 | NS | 0 | benign | 0.49 | tolerated | weakly | highly |
| *CACNA2D4* | 0 | 0 | 3/120548 | SS | undef | undef | undef | undef | na (splicesite) | na (splicesite) |
| *TMED3* | 0 | 0 | 0/121000 | NS | 0.773 | possibly damaging | 0.06 | tolerated | moderately | highly |
| *MYO15A* | 17/12365 | 4/996 | 199/119810 | NS | 0.999 | probably damaging | undef | undef | weakly | highly |
| *STAU1* | 3/13003 | 0 | 16/121402 | NS | 0.911 | possibly damaging | 0.33 | tolerated | weakly | highly |

Candidate variants and their frequency in different databases. Polyphen and SIFT predict the effect of the mutation. Effect NS is non-synonymous, SS splice site. Conserved nucleotide (Nucl) and conserved amino acids (AA) determined the conservation of the altered amino acid (AA). Condel stands for CONsensus DELeteriousness score of non-synonymous single nucleotide variants (SNVs) according to González-Pérez & López-Bigas [57].

https://doi.org/10.1371/journal.pone.0290013.t003

## Discussion

In an attempted to prioritize the 11 identified candidate genes for a possible role in colour agnosia, we have analysed gene function, link to visual perception, link to cortical specialization, conservation of the nucleotide or amino acid, frequency worldwide or in the Dutch population (Table 3) and its presence in previously linked regions for other cortical disorders for example prosopagnosia or dyslexia [4].

None of the identified genes or its variants was present amongst previously identified genes or loci related to dyslexia, dyscalculi or prosopagnosia. Linked regions were studied on OMIM

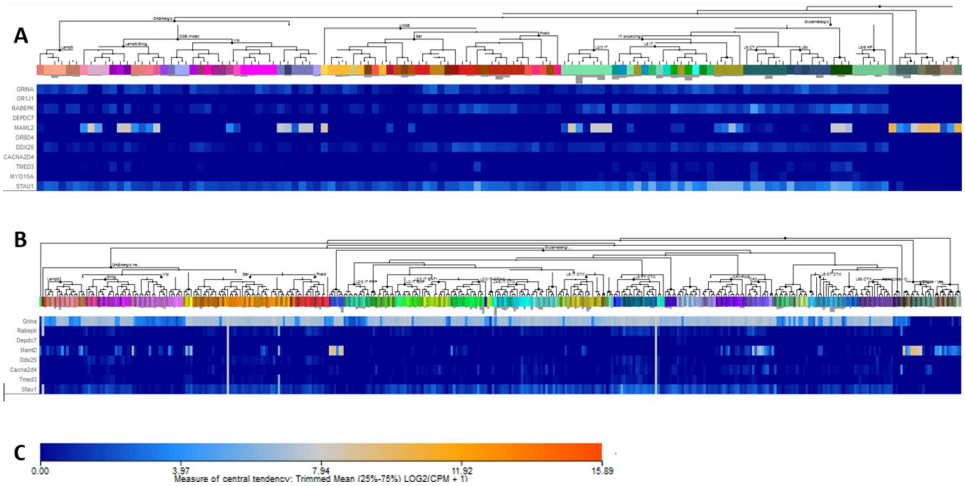


**Fig 4. Expression of the candidate genes in different neuronal and non-neuronal cell types in the human brain (M1 motor cortex) and the mouse whole cortex and hippocampus.** Data were obtained from the single-cell RNA-seq cell types databases of the Allen Brain Institute https://portal.brain-map.org/atlases-and-data/rnaseq). Expression levels are plotted under the neuronal and nonneuronal cell types identified in theses samples. Human olfactory receptors *OR1J1* and *OR8D4* lack identifiable orthologues in the mouse. Panel A: Human. Panel B: Mouse. Panel C: Intensity scale 0–15.89.

https://doi.org/10.1371/journal.pone.0290013.g004

(www.omim.org/). GO-analysis identified that the *calcium channel*, *voltage-dependent*, *alpha 2/delta subunit 4 (Cav1.4)* gene *CACNA2D4* and *MYO15A* were involved in visual perception, which makes *CACNA2D4 and MYO15A* candidate genes of interest.

*CACNA2D4* encodes the α2δ4 subunit of the photoreceptor voltage-gated calcium channels (Cav1.4), which modulate glutamate release from the photoreceptors to the bipolar cells. The CACNA2D4 mutation is a splice-site mutation and its role on the Cav1.4 protein function is unclear. Mutations in the human *CACNA2D4* gene are involved in recessive cone dystrophy [27, 28]. Mice with a premature stop mutation in *Cacna2d4* show abnormal morphology of ribbon synapses in the rods and cones [29]. In mice loss of *Cacna2d4* abolished rod synaptogenesis and synaptic transmission and disrupted mGluR6 clustering [30]. This suggests that CACN2D4 is involved in visual perception by the eye, but it does not provide an argument for its involvement in higher order cortical specialisation and visual perception. There was no indication that the family members with developmental colour agnosia suffered from an ophthalmic problem. This may also suggest that the splice-site mutation that we identified is not deleterious. Furthermore, *CACNA2D4* has been implicated in autism spectrum disorders [31], and a deletion in the *CACNA2D4* gene was found in a patient with bipolar disorder, but it is unknown if this patient suffers with vision problems [32]. Our attempts to trace this patient for developmental colour agnosia testing failed. Studies of other CACNA subtypes showed that thermal pain and tactile stimulation in the *Cacna2d3* mutant mice triggered strong cross-activation of brain regions involved in vision, olfaction, and hearing. This study suggested that this knockout model could be a model for synaesthesia [33], which is a disorder related to developmental colour agnosia [34].

*MYO15A* mutations are associated with non-syndromic hearing loss. Deafness due to its critical role for the formation of stereocilia in cochlear hair cells [35]. Recessive mutations lead to autosomal recessive non-syndromic hearing loss [36]. *MYO15A* mutations are associated with the Usher syndrome having affected hearing [37]. Visual perception is also affected In Usher syndrome from the age of 10 years onwards. Vision loss is caused by retinopathia which is due to degeneration of retina cells, usually the rods cells.

Since no direct link to visual perception was found for the other genes, their possible function in the (developing) brain was considered for these genes. It has been indicated that glutamate receptor, ionotropic, N-methyl D-aspartate-associated protein 1 (glutamate binding) (*GRINA*) is involved in nervous system development and disease mainly through signalling mechanisms of neuronal survival [38]. Upregulation of *GRINA* transcripts was observed in post-mortem brains of patients with major depressive disorder, supporting a role in brain functions [39]. *Grina* knock-out (KO) mice do not display an obvious phenotype [40]. This KO study showed that the effects of the *GRINA* gene are probably subtle. Since it is likely that effects on higher order visual perception will not be evident in mice, *GRINA* remains a potentially interesting candidate gene for consideration of a role in developmental colour agnosia. The effect of the mutation is probably damaging or deleterious (SIFT) and the site of mutation is highly conserved for nucleotide sequence and amino acid motif.

*DDX25 (DEAD (Asp-Glu-Ala-Asp) box polypeptide 25)* encodes a member of the large DEAD-box RNA helicases. Members of this protein family share high structural conservation and are generally involved in developmental processes such as gametogenesis, germ cell specification, and stem cell biology. Data on roles of DDX proteins in the brain are scarce. However, recently two members have been implicated in brain processes. Firstly, in a family with orofaciodigital syndrome type V a homozygous frameshift deletion in *DDX59* (c.185del: p. Phe62fs*13) has been reported [41]. The neurological phenotypes of this syndrome include developmental delay, cognitive impairment, diffuse white matter abnormalities associated with cortical and subcortical ischemic events [41]. Further research in *Drosphila* showed

impaired development of peripheral and central nervous system upon loss-of-function of *DDX59*, supporting a conserved role of this DEAD-box RNA helicase in neurological function. Secondly, mutations in *DDX3X* cause neurodevelopmental abnormalities in females, including intellectual disability, cortical malformations, autism and epilepsy [42]. In this study it was shown that in vivo depletion of Ddx3x in mice reduced neuronal differentiation and impaired corticogenesis [42].

A role of DDX25 in the brain has not been studied. Sofar *DDX25* has been implicated in spermatogenesis and primordial germ cell development [43, 44]. Polymorphisms in the *DDX25* gene have been found that alter protein function [45]. During our expression analyses of DDX25 we found significant expression in the brain. The Allen Brain Atlas Data Portal (http://casestudies.brain-map.org/celltax#section_explorea) showed expression of *Ddx25* in mouse cerebral cortex, nucleus accumbens, several thalamic and hypothalamic nuclei, locus coeruleus, raphe nucleus, inferior olivary complex, and absence in globus pallidus, and most of the midbrain and brain stem. Further exploration of mouse cortical gene expression of the data of [22] through the Single Cell Portal (https://portals.broadinstitute.org/single_cell) showed expression of *Ddx25* in all subtypes of interneurons and pyramidal cells. Transcripts were absent in glial cells (not shown). Mining of more recent data from single-cell transcriptomics [20] showed that expression of *DDX25* in human and mouse cortex is relatively low and is predominating in somatostatin- and parvalbumin- expressing interneurons, and in several types of pyramidal neurons, mostly located in layers 5–6 (dataset human M1; Fig 4A). In the dataset 'Multiple cortical areas' no evident expression was detected. There was no clear age-related change in human brain samples (Fig 3). In mouse single-cell data sets there was very low expression in parvalbumin-expressing interneurons and layer 5 pyramidal neurons (Fig 4B). Overall, *DDX25* appears a gene with low and restricted expression in the adult cortex. Since it is part of a little-studied family causing severe neurological problems, as in the case of *DDX3A* and *DDX59* mutations, *DDX25* should still be considered a potential candidate gene for involvement in developmental colour agnosia.

*Staufen double-stranded RNA binding protein 1* gene *STAU1* carried a possibly damaging (Polyphen) and tolerated (SIFT) mutation in a highly conserved amino acid motif. Staufen1 is a key protein involved in the local translation of mRNA in the dendrite and is involved in protein synaptic transmisson. Further, Staufen 1 was indispensable for self-renewal and differentiation of neuronal precursor cells in vitro. Cultured neurons from *Stau1* knockout mice showed reduced dendritic trees and developed fewer synapses, but the mice did not show any obvious defects in brain development [46]. We note that recently a molecular and functional relationship between Stau1 and DEAD-box RNA helicases (Ddx5/17) was established in a complex with the Kruppel-like factor Klf4 [47]. It was shown that this Klf4/Stau1/Ddx5/7 protein complex regulates neurogenesis-associated mRNAs and plays a role in mammalian corticogenesis. Furthermore, local regulatory networks containing *STAU1* have been identified in cognitive decline in older adults [48]. In accord with a neuronal role, *STAU1* appeared expressed in virtually all types of cortical neurons in mouse and man, but not in non-neuronal cells of the cerebral cortex.

The *Mastermind-like 2* (*MAML2*) gene, encoding a transcriptional activator of the Notch signalling pathway [49], has been implicated in cancers, but has no known function in the nervous system. The effect of the found mutation is probably damaging in Polyphen and tolerated in SIFT. The nucleotide and amino acid sequence is moderate and highly conserved, respectively. In this study *MAML2* is notable since its brain expression is increased during development (age 0.1–0.5 years) in comparison to older ages (Fig 3). Interestingly, it displayed highest expression by several non-neuronal cell types. In the human cortex these were: oligodendrocyte progenitor cell L1-6 PDGFRA COL20A1 (trimmed mean expression level 10.2), several

types of astrocytes (level 9.8–10.3) and microglia (level 10.9) (Fig 4). Neuronal expression of MAML2 at appreciable level occurred in three subtype of inhibitory neurons: inhibitory neuron L1 Pax6 Mir 101–1 (level: 8.2), inhibitory neuron L1-2 VIP WNT4 (level: 8.54), inhibitory neuron L1-6 SST NPY (level 8.67). Two excitatory cell types expressed MAML2: L3 LINC00507 and L3 FEZF2 (respectively at level 8.58 and 7.08). In a single- dataset of the mouse cortex and hippocampus, *Maml2* gene was highest expressed in cells of the dentate gyrus and CA region (Fig 4). The Allen Mouse Brain Atlas confirmed the selective high expression of *Maml2* in the dentate gyrus.

*RABEPK (Rab9 effector protein with Kelch motifs)* belonged to a small set of genes emerging in genome-wide association studies of opioid use disorder [50]. However, the gene has not been studied further to any extent. It is thought to participate in protein transport in the trans-Golgi network. The effect of the mutations is a probably damaging in Polyphen and deleterious in SIFT and the conservation is high for both sequences. Expression of the *RABEPK* gene is not detectable in single-cell data sets of the human cortex and in very low level in several types of interneurons and pyramidal cells in the mouse cortex and hippocampus (Fig 4).

The expression of *transmembrane emp24 protein transport domain containing 3* (*TMED3*) is noticeable in its increased between the age of 0.3–8 years in the human prefrontal cortex (Fig 3). *TMED3* expression is assigned to all interneurons and pyramidal cells in the mouse cortex (Single Cell Portal; [22]), but displays very low to no expression in more recent human and mouse datasets. TMED3 participates in tumor progression, but functions of TMED3 in the brain have not been described. Interestingly, it has been proposed that in tumors TMED3 promotes endogenous Wnt-Tcf activity, which is an important pathway in brain development, and Il11/Stat3 signalling [51, 52]. The effect of the mutation is possibly damaging in Polyphen and tolerated in SIFT and conservation is moderate for nucleotide and highly conserved for amino acid sequence (Table 2).

The effect of the mutation found in the *DEPDC7 (DEP domain-containing 7)* gene is a possibly damaging one in Polyphen and tolerated in SIFT (Table 2). Brain expression of *DEPDC7* was not detectable. However, it has been suggested that *DEPDC7* DNA hypomethylation may be associated with depression [53]. The biological function of the protein encoded by the *DEPDC7* (DEP domain-containing 7) gene is poorly understood. The DEPDC7 protein participates in gene regulation by NF-κB [54]. It has been shown that it inhibits tumor growth [55]. The gene has been detected amongst nine genes in a microdeletion in a patient with cryptorchidism and azoospermia [56].

No data are available on the function of olfactory receptors *OR1J1 (olfactory receptor*, *family 1*, *subfamily J*, *member 1)* and *OR8D4*. Expression of ORs has been observed in other tissues than olfactory neurons. *OR8D4* has been encountered as a risk gene of systemic lupus erythematosus. The mutation for *OR1J1* is benign for Polyphen and tolerated for SIFT. The mutation in *OR8D4* is benign in Polyphen and deleterious in SIFT.

Taken together, this study is the first attempt to pinpoint genomic regions and genetic variants in developmental colour agnosia, a cognitive trait affecting the understanding of colours. This study was made possible by the finding and characterization of an unique family carrying this trait [7, 9]. We assumed that developmental colour agnosia is an extremely rare trait. Additional subjects were not found since initiation of this study in 2012. Since developmental colour agnosia is not a disorder that requires medical or psychological attention, it will generally stay unnoticed, which hampers the estimation of prevalence. Consequently, the small number of affected subjects is a main limitation of this study.

In addition to number of subjects, this study is also limited by the assumption that developmental colour agnosia is inherited in an autosomal dominant manner with complete penetrance, based on the segregation pattern in the family. Furthermore, the exomes were analysed

in 2012 and since then the quality of capture and sequencing have improved. In addition, we cannot exclude the involvement of genomic rearrangement or mutations in noncoding parts of the genome which we would not have captured using exome sequencing. Within these limitations this study indicates 11 genes that link to the trait. Amongst these there are candidate that have been implicated in neural processes and functions (*CACNA2D4*, *MYO15A*, *DDX25*, *GRINA*), that have an indirect link to brain function or development (*STAU1*, *MAML2*, *TMED3*, *RABEPK*), while others remain unlikely due to lack of brain expression, involvement of non-neural traits (*OR1J1*, *OR8D4*, *DEPDC7*)

In summary, we identified 19 genomic regions and 11 coding variants in hereditary colour agnosia by exome sequencing. Since replication is not possible yet due to the uniqueness of this identified family we cannot pinpoint the causal variant at this stage. Further research is required to identify the genetic origins of developmental colour agnosia for which the identification of new families with this trait is a prerequisite.

## Author Contributions

**Conceptualization:** Tanja C. W. Nijboer, Martine J. van Zandvoort, Eva H. Brilstra, J. Peter H. Burbach.

**Data curation:** Ellen V. S. Hessel, Gijs W. van Haaften, Bobby P. C. Koeleman, J. Peter H. Burbach.

**Formal analysis:** Tanja C. W. Nijboer, Ellen V. S. Hessel, Gijs W. van Haaften, Martine J. van Zandvoort, Peter J. van der Spek, Christine Troelstra, Bert van der Zwaag, J. Peter H. Burbach.

**Funding acquisition:** Martine J. van Zandvoort, J. Peter H. Burbach.

**Investigation:** Tanja C. W. Nijboer, Gijs W. van Haaften, Bobby P. C. Koeleman, Bert van der Zwaag, Eva H. Brilstra.

**Methodology:** Gijs W. van Haaften, Carolien G. F. de Kovel, Bobby P. C. Koeleman, Eva H. Brilstra, J. Peter H. Burbach.

**Project administration:** Tanja C. W. Nijboer, Ellen V. S. Hessel, Gijs W. van Haaften, J. Peter H. Burbach.

**Resources:** Tanja C. W. Nijboer, Gijs W. van Haaften, Bobby P. C. Koeleman.

**Supervision:** Carolien G. F. de Kovel, Bobby P. C. Koeleman, Bert van der Zwaag, Eva H. Brilstra, J. Peter H. Burbach.

**Validation:** Tanja C. W. Nijboer, Carolien G. F. de Kovel, Eva H. Brilstra, J. Peter H. Burbach.

**Visualization:** Ellen V. S. Hessel, J. Peter H. Burbach.

**Writing – original draft:** Tanja C. W. Nijboer, J. Peter H. Burbach.

**Writing – review & editing:** Tanja C. W. Nijboer, Gijs W. van Haaften, J. Peter H. Burbach.

## References

1. Ayala R, Shu T, Tsai L-H. Trekking across the brain: the journey of neuronal migration. Cell [Internet]. 2007 Jan 12 [cited 2012 Oct 29]; 128(1):29–43. Available from: http://www.ncbi.nlm.nih.gov/pubmed/17218253 https://doi.org/10.1016/j.cell.2006.12.021 PMID: 17218253
2. Sossey-Alaoui K, Hartung AJ, Guerrini R, Manchester DK, Posar A, Puche-Mira A, et al. Human doublecortin (DCX) and the homologous gene in mouse encode a putative Ca2+-dependent signaling protein which is mutated in human X-linked neuronal migration defects. Hum Mol Genet. 1998; 7(8):1327–32. https://doi.org/10.1093/hmg/7.8.1327 PMID: 9668176

3. Pilz DT, Matsumoto N, Minnerath S, Mills P, Gleeson JG, Allen KM, et al. LIS1 and XLIS (DCX) mutations cause most classical lissencephaly, but different patterns of malformation. Hum Mol Genet. 1998; 7(13):2029–37. https://doi.org/10.1093/hmg/7.13.2029 PMID: 9817918

4. Mitchell KJ. Curiouser and curiouser: genetic disorders of cortical specialization. Curr Opin Genet Dev [Internet]. 2011 Jun [cited 2012 Nov 12]; 21(3):271–7. Available from: http://www.ncbi.nlm.nih.gov/pubmed/21296568 https://doi.org/10.1016/j.gde.2010.12.003 PMID: 21296568

5. Hu WF, Chahrour MH, Walsh CA. The diverse genetic landscape of neurodevelopmental disorders. Annu Rev Genomics Hum Genet. 2014; 15:195–213. https://doi.org/10.1146/annurev-genom-090413-025600 PMID: 25184530

6. De Vreese LP. Two systems for colour-naming defects: Verbal disconnection vs colour imagery disorder. Neuropsychologia [Internet]. 1991 [cited 2021 Mar 23]; 29(1):1–18. Available from: https://pubmed.ncbi.nlm.nih.gov/2017304/ https://doi.org/10.1016/0028-3932(91)90090-u PMID: 2017304

7. Nijboer TCW, van Zandvoort MJE, de Haan EHF. A familial factor in the development of colour agnosia. Neuropsychologia [Internet]. 2007 Apr 9 [cited 2012 Dec 3]; 45(8):1961–5. Available from: http://www.ncbi.nlm.nih.gov/pubmed/17337019 https://doi.org/10.1016/j.neuropsychologia.2007.01.021 PMID: 17337019

8. Nijboer TCW, van Zandvoort MJE, de Haan EHF. Covert colour processing in colour agnosia. Neuropsychologia [Internet]. 2006 Jan [cited 2012 Dec 3]; 44(8):1437–43. Available from: http://www.ncbi.nlm.nih.gov/pubmed/16420956 https://doi.org/10.1016/j.neuropsychologia.2005.12.004 PMID: 16420956

9. van Zandvoort MJE, Nijboer TCW, de Haan E. Developmental colour agnosia. Cortex. 2007; 43 (6):750–7. https://doi.org/10.1016/s0010-9452(08)70503-3 PMID: 17710826

10. De Renzi E. Disorders of visual recognition [Internet]. Vol. 20, Seminars in Neurology. Semin Neurol; 2000 [cited 2021 Mar 23]. p. 479–85. Available from: https://pubmed.ncbi.nlm.nih.gov/11149704/ https://doi.org/10.1055/s-2000-13181 PMID: 11149704

11. Nijboer TCW, van Der Smagt MJ, van Zandvoort MJE, De Haan EHF. Colour agnosia impairs the recognition of natural but not of non-natural scenes. Cogn Neuropsychol. 2007 Mar; 24(2):152–61. https://doi.org/10.1080/02643290600989541 PMID: 18416486

12. Vermeesch JR, Fiegler H, de Leeuw N, Szuhai K, Schoumans J, Ciccone R, et al. Guidelines for molecular karyotyping in constitutional genetic diagnosis. Eur J Hum Genet [Internet]. 2007 Nov [cited 2021 Mar 23]; 15(11):1105–14. Available from: https://pubmed.ncbi.nlm.nih.gov/17637806/ https://doi.org/10.1038/sj.ejhg.5201896 PMID: 17637806

13. Van Binsbergen E, Hochstenbach R, Giltay J, Swinkels M. Unstable transmission of a familial complex chromosome rearrangement. Am J Med Genet Part A [Internet]. 2012 Nov [cited 2021 Mar 23]; 158 A (11):2888–93. Available from: https://pubmed.ncbi.nlm.nih.gov/22987625/ https://doi.org/10.1002/ajmg.a.35580 PMID: 22987625

14. Carr IM, Johnson CA, Markham AF, Toomes C, Bonthron DT, Sheridan EG. DominantMapper: Rule-based analysis of SNP data for rapid mapping of dominant diseases in related nuclear families. Hum Mutat [Internet]. 2011 Dec [cited 2021 Mar 23]; 32(12):1359–66. Available from: https://pubmed.ncbi.nlm.nih.gov/21905167/ https://doi.org/10.1002/humu.21597 PMID: 21905167

15. Harakalova M, Van Harssel JJT, Terhal PA, Van Lieshout S, Duran K, Renkens I, et al. Dominant missense mutations in ABCC9 cause Cantúsyndrome. Nat Genet. 2012 Jul; 44(7):793–6.

16. Harakalova M, Mokry M, Hrdlickova B, Renkens I, Duran K, Van Roekel H, et al. Multiplexed array-based and in-solution genomic enrichment for flexible and cost-effective targeted next-generation sequencing. Nat Protoc [Internet]. 2011 Dec [cited 2021 Mar 23]; 6(12):1870–86. Available from: https://pubmed.ncbi.nlm.nih.gov/22051800/ https://doi.org/10.1038/nprot.2011.396 PMID: 22051800

17. Nijman IJ, Mokry M, Van Boxtel R, Toonen P, De Bruijn E, Cuppen E. Mutation discovery by targeted genomic enrichment of multiplexed barcoded samples. Nat Methods. 2010 Nov; 7(11):913–5. https://doi.org/10.1038/nmeth.1516 PMID: 20953175

18. Visser WE, Swagemakers SMA, Ozgur Z, Schot R, Verheijen FW, van Ijcken WFJ, et al. Transcriptional profiling of fibroblasts from patients with mutations in MCT8 and comparative analysis with the human brain transcriptome. Hum Mol Genet [Internet]. 2010 Aug 12 [cited 2021 Mar 24]; 19(21):4189–200. Available from: https://pubmed.ncbi.nlm.nih.gov/20705735/ https://doi.org/10.1093/hmg/ddq337 PMID: 20705735

19. Stubbs A, McClellan EA, Horsman S, Hiltemann SD, Palli I, Nouwens S, et al. Huvariome: a web server resource of whole genome next-generation sequencing allelic frequencies to aid in pathological candidate gene selection. J Clin Bioinforma [Internet]. 2012 [cited 2021 Mar 24]; 2(1):19. Available from: https://pubmed.ncbi.nlm.nih.gov/23164068/ https://doi.org/10.1186/2043-9113-2-19 PMID: 23164068

20. Hodge RD, Bakken TE, Miller JA, Smith KA, Barkan ER, Graybuck LT, et al. Conserved cell types with divergent features in human versus mouse cortex. Nature. 2019; 573(7772):61–8. https://doi.org/10.1038/s41586-019-1506-7 PMID: 31435019

21. Tasic B, Yao Z, Graybuck LT, Smith KA, Nguyen TN, Bertagnolli D, et al. Shared and distinct transcriptomic cell types across neocortical areas. Nature. 2018 Nov 1; 563(7729):72–8. https://doi.org/10.1038/s41586-018-0654-5 PMID: 30382198

22. Tasic B, Menon V, Nguyen TN, Kim TK, Jarsky T, Yao Z, et al. Adult mouse cortical cell taxonomy revealed by single cell transcriptomics. Nat Neurosci [Internet]. 2016 Jan 27; 19(2):335–46. Available from: https://doi.org/10.1038/nn.4216 PMID: 26727548

23. Altshuler DL, Durbin RM, Abecasis GR, Bentley DR, Chakravarti A, Clark AG, et al. A map of human genome variation from population-scale sequencing. Nature [Internet]. 2010 Oct 28 [cited 2021 Mar 27]; 467(7319):1061–73. Available from: https://pubmed.ncbi.nlm.nih.gov/20981092/ https://doi.org/10.1038/nature09534 PMID: 20981092

24. Francioli LC, Menelaou A, Pulit SL, Van Dijk F, Palamara PF, Elbers CC, et al. Whole-genome sequence variation, population structure and demographic history of the Dutch population. Nat Genet. 2014; 46(8):818–25. https://doi.org/10.1038/ng.3021 PMID: 24974849

25. Boomsma DI, Wijmenga C, Slagboom EP, Swertz MA, Karssen LC, Abdellaoui A, et al. The Genome of the Netherlands: Design, and project goals. Eur J Hum Genet [Internet]. 2014 Feb [cited 2021 Mar 27]; 22(2):221–7. Available from: https://pubmed.ncbi.nlm.nih.gov/23714750/ https://doi.org/10.1038/ejhg.2013.118 PMID: 23714750

26. Erikson GA, Deshpande N, Kesavan BG, Torkamani A. SG-ADVISER CNV: Copy-number variant annotation and interpretation. Genet Med. 2015 Sep 2; 17(9):714–8. https://doi.org/10.1038/gim.2014.180 PMID: 25521334

27. Wycisk KA, Zeitz C, Feil S, Wittmer M, Forster U, Neidhardt J, et al. Mutation in the auxiliary calcium-channel subunit CACNA2D4 causes autosomal recessive cone dystrophy. Am J Hum Genet. 2006; 79 (5):973–7. https://doi.org/10.1086/508944 PMID: 17033974

28. Ba-Abbad R, Arno G, Carss K, Stirrups K, Penkett CJ, Moore AT, et al. Mutations in CACNA2D4 cause distinctive retinal dysfunction in humans. Ophthalmology [Internet]. 2016 Mar 1 [cited 2021 Mar 25]; 123 (3):668–671.e2. Available from: https://pubmed.ncbi.nlm.nih.gov/26560832/ https://doi.org/10.1016/j.ophtha.2015.09.045 PMID: 26560832

29. Wycisk KA, Budde B, Feil S, Skosyrski S, Buzzi F, Neidhardt J, et al. Structural and functional abnormalities of retinal ribbon synapses due to Cacna2d4 mutation. Investig Ophthalmol Vis Sci. 2006 Aug; 47(8):3523–30. https://doi.org/10.1167/iovs.06-0271 PMID: 16877424

30. Wang Y, Fehlhaber KE, Sarria I, Cao Y, Ingram NT, Guerrero-Given D, et al. The Auxiliary Calcium Channel Subunit α2δ4 Is Required for Axonal Elaboration, Synaptic Transmission, and Wiring of Rod Photoreceptors. Neuron [Internet]. 2017 Mar 22 [cited 2021 Mar 25]; 93(6):1359–1374.e6. Available from: https://pubmed.ncbi.nlm.nih.gov/28262416/

31. Liao X, Liao X, Li Y. Genetic associations between voltage-gated calcium channels and autism spectrum disorder: A systematic review [Internet]. Vol. 13, Molecular Brain. BioMed Central Ltd.; 2020 [cited 2021 Mar 25]. Available from: https://pubmed.ncbi.nlm.nih.gov/32571372/ https://doi.org/10.1186/s13041-020-00634-0 PMID: 32571372

32. Van Den Bossche MJ, Strazisar M, De Bruyne S, Bervoets C, Lenaerts AS, De Zutter S, et al. Identification of a CACNA2D4 deletion in late onset bipolar disorder patients and implications for the involvement of voltage-dependent calcium channels in psychiatric disorders. Am J Med Genet Part B Neuropsychiatr Genet. 2012 Jun; 159 B(4):465–75. https://doi.org/10.1002/ajmg.b.32053 PMID: 22488967

33. Neely GG, Hess A, Costigan M, Keene AC, Goulas S, Langeslag M, et al. A genome-wide Drosophila screen for heat nociception identifies α2δ3 as an evolutionarily conserved pain gene. Cell [Internet]. 2010 Nov 12 [cited 2012 Nov 13]; 143(4):628–38. Available from: http://www.pubmedcentral.nih.gov/articlerender.fcgi?artid=3040441&tool=pmcentrez&rendertype=abstract

34. Rich AN, Mattingley JB. Anomalous perception in synaesthesia: A cognitive neuroscience perspective. Nat Rev Neurosci. 2002; 3(1):43–52. https://doi.org/10.1038/nrn702 PMID: 11823804

35. Probst FJ, Fridell RA, Raphael Y, Saunders TL, Wang A, Liang Y, et al. Correction of deafness in shaker-2 mice by an unconventional myosin in a BAC transgene. Science ( 80-) [Internet]. 1998 May 29 [cited 2021 Mar 25]; 280(5368):1444–7. Available from: https://pubmed.ncbi.nlm.nih.gov/9603735/

36. Wang A, Liang Y, Fridell RA, Probst FJ, Wilcox ER, Touchman JW, et al. Association of unconventional myosin MYO15 mutations with human nonsyndromic deafness DFNB3. Science ( 80-) [Internet]. 1998 May 29 [cited 2021 Mar 25]; 280(5368):1447–51. Available from: https://pubmed.ncbi.nlm.nih.gov/9603736/ https://doi.org/10.1126/science.280.5368.1447 PMID: 9603736

37. Baux D, Vaché C, Blanchet C, Willems M, Baudoin C, Moclyn M, et al. Combined genetic approaches yield a 48% diagnostic rate in a large cohort of French hearing-impaired patients. Sci Rep. 2017 Dec 1; 7(1).

38. Chen K, Yang LN, Lai C, Liu D, Zhu L-Q. Role of Grina/Nmdara1 in the Central Nervous System Diseases. Curr Neuropharmacol [Internet]. 2021 Mar 3 [cited 2021 Mar 25]; 18(9):861–7. Available from: https://pubmed.ncbi.nlm.nih.gov/32124700/

39. Goswami DB, Jernigan CS, Chandran A, Iyo AH, May WL, Austin MC, et al. Gene expression analysis of novel genes in the prefrontal cortex of major depressive disorder subjects. Prog Neuro-Psychopharmacology Biol Psychiatry [Internet]. 2013 Jun 3 [cited 2021 Mar 25]; 43:126–33. Available from: https://pubmed.ncbi.nlm.nih.gov/23261523/ https://doi.org/10.1016/j.pnpbp.2012.12.010 PMID: 23261523

40. Nielsen JA, Chambers MA, Romm E, Lee LYH, Berndt JA, Hudson LD. Mouse transmembrane BAX inhibitor motif 3 (Tmbim3) encodes a 38 kDa transmembrane protein expressed in the central nervous system. Mol Cell Biochem [Internet]. 2011 Nov [cited 2021 Mar 25]; 357(1–2):73–81. Available from: https://pubmed.ncbi.nlm.nih.gov/21614515/ https://doi.org/10.1007/s11010-011-0877-3 PMID: 21614515

41. Salpietro V, Efthymiou S, Manole A, Maurya B, Wiethoff S, Ashokkumar B, et al. A loss-of-function homozygous mutation in DDX59 implicates a conserved DEAD-box RNA helicase in nervous system development and function. Hum Mutat [Internet]. 2018 Feb 1 [cited 2021 Mar 25]; 39(2):187–92. Available from: https://pubmed.ncbi.nlm.nih.gov/29127725/ https://doi.org/10.1002/humu.23368 PMID: 29127725

42. Lennox AL, Hoye ML, Jiang R, Johnson-Kerner BL, Suit LA, Venkataramanan S, et al. Pathogenic DDX3X Mutations Impair RNA Metabolism and Neurogenesis during Fetal Cortical Development. Neuron. 2020 May 6; 106(3):404–420.e8. https://doi.org/10.1016/j.neuron.2020.01.042 PMID: 32135084

43. Tsai-Morris CH, Sheng Y, Lee E, Lei KJ, Dufau ML. Gonadotropin-regulated testicular RNA helicase (GRTH/Ddx25) is essential for spermatid development and completion of spermatogenesis. Proc Natl Acad Sci U S A. 2004 Apr 27; 101(17):6373–8. https://doi.org/10.1073/pnas.0401855101 PMID: 15096601

44. Kavarthapu R, Anbazhagan R, Raju M, Morris CHT, Pickel J, Dufau ML. Targeted knock-in mice with a human mutation in GRTH/DDX25 reveals the essential role of phosphorylated GRTH in spermatid development during spermatogenesis. Hum Mol Genet. 2019 Aug 1; 28(15):2561–72. https://doi.org/10.1093/hmg/ddz079 PMID: 31009948

45. Tsai-Morris CH, Koh E, Sheng Y, Maeda Y, Gutti R, Namiki M, et al. Polymorphism of the GRTH/DDX25 gene in normal and infertile Japanese men: A missense mutation associated with loss of GRTH phosphorylation. Mol Hum Reprod [Internet]. 2007 Dec [cited 2021 Mar 25]; 13(12):887–92. Available from: https://pubmed.ncbi.nlm.nih.gov/17848414/ https://doi.org/10.1093/molehr/gam065 PMID: 17848414

46. Vessey JP, Macchi P, Stein JM, Mikl M, Hawker KN, Vogelsang P, et al. A loss of function allele for murine Staufen1 leads to impairment of dendritic Staufen1-RNP delivery and dendritic spine morphogenesis. Proc Natl Acad Sci U S A [Internet]. 2008 Oct 21 [cited 2021 Mar 25]; 105(42):16374–9. Available from: https://pubmed.ncbi.nlm.nih.gov/18922781/ https://doi.org/10.1073/pnas.0804583105 PMID: 18922781

47. Moon BS, Bai J, Cai M, Liu C, Shi J, Lu W. Kruppel-like factor 4-dependent Staufen1-mediated mRNA decay regulates cortical neurogenesis. Nat Commun [Internet]. 2018 Dec 1 [cited 2021 Mar 25]; 9(1). Available from: https://pubmed.ncbi.nlm.nih.gov/29374155/

48. Tasaki S, Gaiteri C, Mostafavi S, Yu L, Wang Y, De Jager PL, et al. Multi-omic directed networks describe features of gene regulation in aged brains and expand the set of genes driving cognitive decline. Front Genet [Internet]. 2018 Aug 9 [cited 2021 Mar 25];9(AUG). Available from: https://pubmed.ncbi.nlm.nih.gov/30140277/ https://doi.org/10.3389/fgene.2018.00294 PMID: 30140277

49. Just Ribeiro M, Wallberg A. Transcriptional Mechanisms by the Coregulator MAML1. Curr Protein Pept Sci [Internet]. 2009 Oct 17 [cited 2021 Mar 25]; 10(6):570–6. Available from: https://pubmed.ncbi.nlm.nih.gov/19751190/ https://doi.org/10.2174/138920309789630543 PMID: 19751190

50. Kember RL, Vickers-Smith R, Xu H, Toikumo S, Niarchou M, Zhou H, et al. Cross-ancestry meta-analysis of opioid use disorder uncovers novel loci with predominant effects in brain regions associated with addiction. Nat Neurosci. 2022 Oct; 25(10):1279–1287. https://doi.org/10.1038/s41593-022-01160-z Epub 2022 Sep 28. Available from: https://pubmed.ncbi.nlm.nih.gov/36171425/ PMID: 36171425

51. Duquet A, Melotti A, Mishra S, Malerba M, Seth C, Conod A, et al. A novel genome-wide in vivo screen for metastatic suppressors in human colon cancer identifies the positive WNT - TCF pathway modulators TMED 3 and SOX 12. EMBO Mol Med [Internet]. 2014 Jul [cited 2021 Mar 25]; 6(7):882–901. Available from: https://pubmed.ncbi.nlm.nih.gov/24920608/ https://doi.org/10.15252/emmm.201303799 PMID: 24920608

52. Zheng H, Yang Y, Han J, Jiang WH, Chen C, Wang MC, et al. TMED3 promotes hepatocellular carcinoma progression via IL-11/STAT3 signaling. Sci Rep [Internet]. 2016 Nov 30 [cited 2021 Mar 25]; 6. Available from: https://pubmed.ncbi.nlm.nih.gov/27901021/ https://doi.org/10.1038/srep37070 PMID: 27901021

53. Córdova-Palomera A, Fatjó-Vilas M, Palma-Gudiel H, Blasco-Fontecilla H, Kebir O, Fañanás L. Further evidence of DEPDC7 DNA hypomethylation in depression: A study in adult twins. Eur Psychiatry [Internet]. 2015 Sep 1 [cited 2021 Mar 25]; 30(6):715–8. Available from: https://pubmed.ncbi.nlm.nih.gov/25952135/ https://doi.org/10.1016/j.eurpsy.2015.04.001 PMID: 25952135

54. D'Andrea EL, Ferravante A, Scudiero I, Zotti T, Reale C, Pizzulo M, et al. The dishevelled, EGL-10 and pleckstrin (DEP) domain-containing protein DEPDC7 binds to CARMA2 and CARMA3 proteins, and regulates NF-κB activation. PLoS One [Internet]. 2014 Dec 26 [cited 2021 Mar 25]; 9(12). Available from: https://pubmed.ncbi.nlm.nih.gov/25541973/

55. Liao Z, Wang X, Wang X, Li L, Lin D. DEPDC7 inhibits cell proliferation, migration and invasion in hepatoma cells. Oncol Lett [Internet]. 2017 Dec 1 [cited 2021 Mar 25]; 14(6):7332–8. Available from: https://pubmed.ncbi.nlm.nih.gov/29344171/ https://doi.org/10.3892/ol.2017.7128 PMID: 29344171

56. Seabra CM, Quental S, Neto AP, Carvalho F, Gonçalves J, Oliveira JP, et al. A novel Alu-mediated microdeletion at 11p13 removes WT1 in a patient with cryptorchidism and azoospermia. Reprod Biomed Online [Internet]. 2014 [cited 2021 Mar 25]; 29(3):388–91. Available from: https://pubmed.ncbi.nlm.nih.gov/24912414/ https://doi.org/10.1016/j.rbmo.2014.04.017 PMID: 24912414

57. González-Pérez A, López-Bigas N. Improving the assessment of the outcome of nonsynonymous SNVs with a consensus deleteriousness score, Condel. Am J Hum Genet. 2011 Apr 8; 88(4):440–9. https://doi.org/10.1016/j.ajhg.2011.03.004 PMID: 21457909